

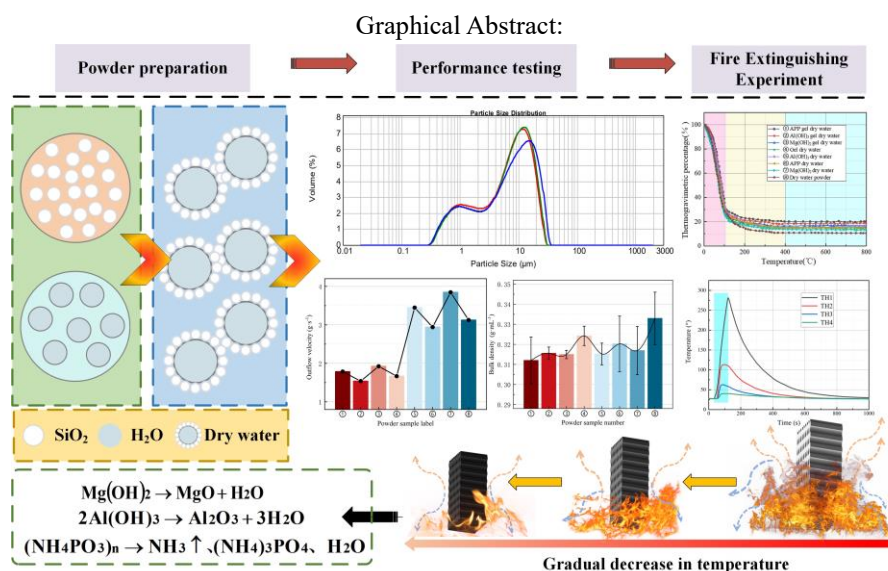
Performance Analysis of Novel Dry-Water Powders for Fire Scenarios in Thermal Insulation Materials

Xuezhao Zheng^{a,b,c}, Jian Song^{a,b,*}, Zhizhe Kou^{a,b},

^a College of Safety Science and Engineering, Xi'an University of Science and Technology, Xi'an 710054, China

^b Xi'an Research Center of National Mine Rescue, Xi'an 710054, China

^c Shaanxi Xikuang Zhitong Technology Co., Ltd., Xi'an, 710086, China



* Corresponding author.

E-mail address: 2220226067@stu.xust.edu.cn (J. Song).

Abstract

To mitigate the casualties and property damage caused by sudden fires in thermal insulation materials, this study employs an integrated approach comprising process optimization, laboratory experiments, and fire scene simulations. The research focuses on the performance of novel dry-water powders under combustion conditions of insulation materials. Specifically, dry-water powders were synthesized using effective fire-extinguishing components such as $\text{Mg}(\text{OH})_2$, $\text{Al}(\text{OH})_3$, APP, along with the surfactant methyl hydrogen silicone oil and the gelling agent Gellan gum, all subjected to modification treatments. The results indicate that the optimal process parameters for preparing dry-water powders are a stirring speed of 24,000 rpm, a stirring time of 5 seconds, and a SiO_2 ratio of 9:100. The $\text{Al}(\text{OH})_3$ gel dry-water powder exhibited good flowability, with an outflow rate of $3.846 \text{ g} \cdot \text{s}^{-1}$ and a repose angle of 27.5° . The novel dry-water powders had low bulk densities, ranging from 0.312 to $0.333 \text{ g} \cdot \text{mL}^{-1}$, with the APP gel dry-water powder having the highest bulk density of $0.333 \text{ g} \cdot \text{mL}^{-1}$. The majority of the dry-water powder particles were within the size range of 1.3 to $250 \mu\text{m}$, with the $\text{Mg}(\text{OH})_2$ gel dry-water powder exhibiting the smallest particle size, where d_{10} was $15.323 \mu\text{m}$, d_{50} was $55.922 \mu\text{m}$, and d_{90} was $216.172 \mu\text{m}$. In flame tests conducted on EPS, XPS, and PU insulation materials, the APP gel dry-water powder, $\text{Mg}(\text{OH})_2$ gel dry-water powder, and $\text{Al}(\text{OH})_3$ gel dry-water powder all exhibited superior fire-extinguishing

Abbreviations: $\text{Mg}(\text{OH})_2$, magnesium hydroxide ; $\text{Al}(\text{OH})_3$, aluminum hydroxide; APP, ammonium polyphosphate; EPS/XPS, polystyrene foam boards; PU, polyurethane foam boards; PSD , particle size distribution.

performance compared to ABC dry powder. Among them, the APP gel dry-water powder demonstrated particularly notable effectiveness in extinguishing fires in EPS and XPS, while the $\text{Al}(\text{OH})_3$ gel dry-water powder also performed well in PU flames. Moreover, the flowability and stability of all three gel dry-water powders were significantly enhanced, effectively reducing the challenges associated with powder filling and simultaneously improving their fire-extinguishing capabilities.

Keywords: Novel dry-water powder, Modifier or modifying agent, Thermal insulation material, Optimal process parameters, Fire extinguishing performance

1. Introduction

In the context of building energy conservation, the increased use of thermal insulation materials has concurrently heightened fire risks. Common organic insulation materials such as polystyrene foam boards (EPS, XPS) and polyurethane foam boards (PU) are highly flammable and release toxic gases, posing safety hazards [1][2]. As one of the most common fire extinguishing agents, dry powder extinguishing agent is suitable for insulation material fire, its particle size is mainly distributed between 10~75 μm , the rate of thermal decomposition is low, the ability to capture free radicals is weak, and the effect of fire extinguishing is poor [3]. Li [4] and others prepared a composite ultrafine dry powder $\text{NH}_4\text{H}_2\text{PO}_4$, and found that the fire extinguishing efficiency has been greatly improved, but because of the very small particle size, moisture resistance, durability and dust hazards limit its further application. Novec 1230 extinguishing agent, as a hotspot of gaseous fire extinguishing agent research in recent years, performs well in electrical fires because of its poor economic and physicochemical properties can not be good. and dust hazards limit its further application. Novec 1230 extinguishing agent, as a research hotspot of gaseous extinguishing agent in recent years, performs well in electrical fires, which cannot be well applied to insulation material fires due to its poor economic and physicochemical properties [5]. Therefore, the selection of efficient and environmentally friendly extinguishing agents is crucial. Dry-water extinguishing agent has become a hot spot of current research due to its high efficiency and environmental friendliness [6].

In 1968, Br  nner et al. [7] first proposed a method for preparing water-containing powders using hydrophobic nano-SiO₂ and water under high-speed dispersion conditions. In 1977, Allan [8] defined this powder as "dry-water," which consists of a dry powder encapsulating tiny liquid droplets with strongly hydrophobic nanoparticles. Dry-water appears fluffy and primarily consists of liquid (>90%) [9]. Compared to hydrated compounds, dry-water powders have a higher water content while maintaining solid-state characteristics [10]. Consequently, dry-water has significant potential for applications in areas such as gas hydrates [11-15], food, pharmaceuticals, cosmetics, and fire extinguishing [16-20].

In the study of the properties of dry-water extinguishing agents, the main way to increase their fire extinguishing properties is through modifications [21-23]. Current modification strategies for dry-water extinguishing agents are mainly concentrated on gelling agent modifications and chemical additive modifications [24]. Tian [25] and others used alkali metal salts to modify dry-water to improve its explosion inhibition effect, laying a solid foundation for the application of alkali metal salt additives in dry-water. Chai et al. [26] investigated the effect of sodium acetate, a metal salt, on the modification of dry-water powders and its impact on the efficiency of fire suppression in wooden stacks. The results indicated that while sodium acetate enhanced the fire-extinguishing efficiency, it also led to structural instability, providing a theoretical basis for research on fire suppression in wooden stacks. Due to the unique core-shell structure of dry-water powders, this structure is prone to damage during transportation, storage, and use, which can significantly impair its fire-extinguishing efficacy. Characterization of flow ability and particle size distribution can provide scientific evidence for studying the dispersion properties of dry-water powders. Experimental results on bulk density can be correlated with the storage performance of dry-water powders. Additionally, analysis of thermal stability can offer a direct assessment of the stability of dry-water powders under various environmental conditions.

Currently, dry-water powder in the field of fire extinguishing applications, scholars at home and abroad through the modification of technology, in the cooling and isolation of fire extinguishing based on the addition of asphyxiation and chemical suppression effect. These enhancements add suffocation and chemical suppression effects to the existing cooling and isolation mechanisms [27-30]. Zheng et al. [31] prepared $\text{Mg}(\text{OH})_2$ gel dry-water powders by adding $\text{Mg}(\text{OH})_2$ and gelled coolants to modify the dry-water powder. The study found a

significant increase in its firefighting efficacy. Wang [32] et al. added sodium bicarbonate and others as modifiers to improve cooling and suppression effects. Their results indicated that potassium bicarbonate and potassium acid oxalate monohydrate exhibited superior free radical suppression. Han et al. [33] successfully prepared standard and gelled ADP dry-water using high-speed mixing technology. Their results showed that the gelled components formed a protective film to prevent re-ignition of wood, while the silica coverage reduced thermal radiation from Class B fire fuels, leading to a faster reduction in fire scene temperatures compared to ABC dry powders.

This study utilized effective fire-extinguishing components including $\text{Mg}(\text{OH})_2$, aluminum hydroxide, ammonium polyphosphate, as well as surfactants such as methyl hydrogen silicone oil and gel agents such as gelling agents, to optimize the preparation parameters for novel dry-water powders, resulting in the formulation of eight different dry-water powders. The prepared dry-water powders were subjected to tests for flowability, bulk density, particle size, and stability. Using a custom-built small-scale dry-water powder fire extinguishing experimental system, the fire-extinguishing effectiveness of five different extinguishing agents on three types of insulation materials was evaluated. This research aimed to investigate the flame suppression performance of dry-water powders, with the objective of applying them to extinguish insulation material fires.

2. Powder preparation

2.1. Principle of Dry-water Powder System Preparation

The preparation mechanism of dry-water powders involves the refinement of aqueous solutions into microscopic droplets under high-speed stirring shear forces. Highly hydrophobic solid powders spontaneously form a robust shell layer at the gas-liquid interface, resulting in a stable core-shell structure. When droplets are mixed with hydrophobic substances, surface tension and electrostatic forces cause the hydrophobic material to spontaneously cover the droplet's outer surface, forming a solid shell layer that isolates the liquid from the external environment, thereby achieving "drying" of the liquid. Fig. 1 illustrates the formation of dry-water.

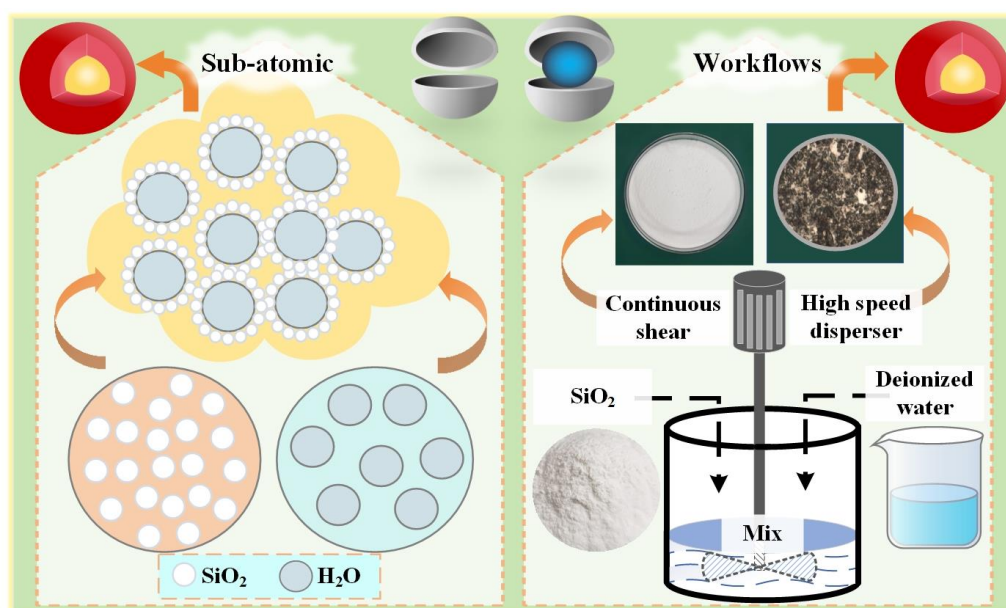


Fig. 1. Schematic diagram of dry-water formation.

2.2. Experimental Materials and Instruments

Deionized water was used as the internal material for the dry-water powders to minimize experimental interference. SiO_2 nanoparticles, known for their high specific surface area and excellent dispersibility, were employed as hydrophobic shell materials to enhance the performance of the dry-water materials. During the modification process, $\text{Mg}(\text{OH})_2$, $\text{Al}(\text{OH})_3$, and ammonium polyphosphate (APP) were selected as fire-extinguishing components. These components suppress flames through mechanisms such as thermal decomposition, which absorbs heat and generates water vapor or gases. Additionally, gelling agents, specifically

Gellan gum, were used to alter the molecular structure through a thermo-reversible phenomenon, thereby strengthening and stabilizing the core-shell structure of the dry-water powders. Furthermore, methyl hydrogen silicone oil was introduced as a surfactant to reduce the difficulty of forming dry-water powders and to isolate the powders from air, further enhancing their fire-extinguishing effectiveness. In the preparation of dry-water powders, an electronic balance ensured the accuracy of material proportions, thus improving experimental reliability; a high-speed disperser accelerated the formation of dry-water powders through high-intensity shear forces; and a polarizing microscope was used to observe the microstructure and assess the quality of the prepared results.

2.3. Determination of optimal preparation parameters

In the preparation of dry-water powders, a literature review and preliminary experiments established optimal conditions of a stirring speed of 24,000 r/min, a stirring time of 5 s, and a SiO_2 : H_2O ratio of 9:100, which resulted in powders with excellent morphology and particle size. Based on these conditions, further single-variable experiments were conducted to investigate the effects of different preparation parameters.

2.3.1. Stirring speed experiment

In the stirring speed study, stirring speeds were adjusted to 12,000, 24,000, and 36,000 r/min across three groups, with the SiO_2 : H_2O ratio kept at 9:100 and stirring time set to 5 s. A comparative experiment was conducted where the only variable was the stirring speed. The appearance of the experimental products is shown in Fig. 2.

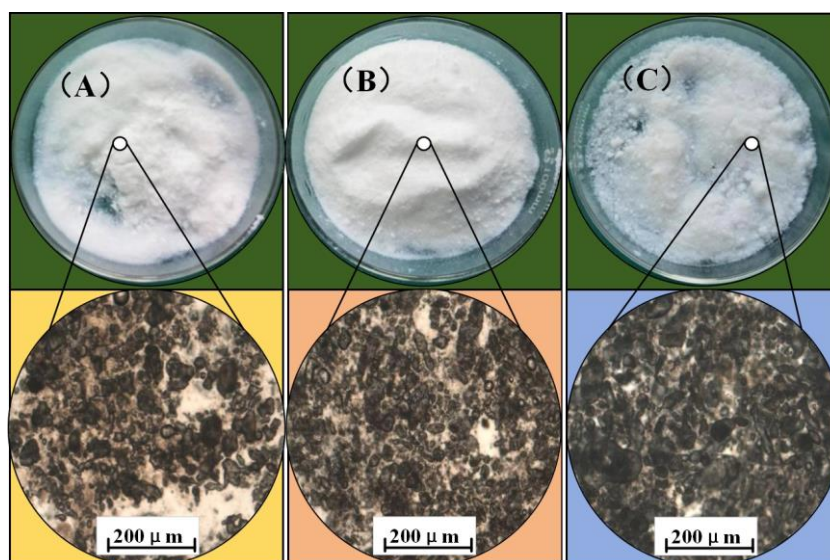


Fig. 2. Appearance and microstructure of dry-water powders at different stirring speeds.(A) 12,000 r/min; (B) 24,000 r/min; (C) 36,000 r/min.

At a stirring speed of 12,000 r/min, significant residual liquid water and silica were observed in the product, indicating insufficient shear force, which resulted in incomplete dispersion of the deionized water and an inability to form a stable core-shell structure. At 36,000 r/min, although the aggregation of silica was reduced, excessive shear force disrupted the formed core-shell structure, resulting in irregular, blocky agglomerates. The optimal stirring speed was found to be 24,000 r/min, at which the product was uniform and free of significant liquid water, exhibiting ideal dry-water powder morphology and good dispersion. Therefore, a stirring speed of 24,000 r/min was selected as the optimal preparation speed for dry-water powders.

2.3.2. Stirring Time Experiment

In the stirring time study, the stirring times were adjusted to 3 s, 5 s, 7 s, and 9 s across four groups, with the SiO_2 : H_2O ratio fixed at 9:100 and the stirring speed set to 24,000 r/min. A comparative experiment was conducted where the only variable was the stirring time. The appearance of the experimental products is shown in Fig. 3.



Fig. 3. Product images of dry-water powders at different stirring times.

This experiment investigated the effects of different stirring times on the product morphology while keeping the stirring speed and SiO_2 : H_2O ratio constant. The results indicate that stirring time significantly affects the structure and stability of the product. As shown in Figure 3, a stirring time that is too short (3 seconds) results in insufficient shear force, leaving a significant amount of liquid at the bottom of the product and preventing the formation of a stable core-shell structure. Conversely, excessively long stirring times (7 and 9 seconds) lead to excessive shear force, which disrupts the formed core-shell structure and causes damage to both the solution and powder particles. In contrast, a stirring time of 5 seconds yields a product with uniform morphology, without significant liquid water or excess silica, indicating adequate mixing and enhanced product stability. Therefore, a stirring time of 5 seconds was selected as the optimal duration for preparing dry-water powders.

2.3.3. Dry-water powder ratio experiment

(1) Investigation of wall material to core material ratio

In the investigation of the wall material to core material ratio, the stirring speed was fixed at 24,000 r/min and the stirring time at 5 s. The SiO_2 : H_2O mass ratios were adjusted to 7:100, 8:100, 9:100, and 10:100 for comparative experiments, as shown in Fig. 4.



Fig. 4. Product images of dry-water powders under different physical ratios.

Through orthogonal experimental design and analysis of the product state, this study investigated the effects of different SiO_2 to deionized water ratios on the characteristics of dry-water powders. As shown in Figure 4, at SiO_2 : H_2O mass ratios of 7:100 and 8:100, residual liquid water was observed at the bottom of the product, attributed to insufficient silica content. When the ratio was increased to 9:100, the liquid water disappeared, indicating that the silica was sufficient to completely encapsulate the droplets. However, at a ratio of 10:100, the product volume increased and excess silica was present. Comprehensive analysis showed that at a SiO_2 : H_2O mass ratio of 9:100, the product exhibited an ideal powder appearance and uniform particle size. Therefore, the optimal preparation parameters were determined to be a stirring speed of 24,000 r/min, a stirring time of 5 seconds, and a SiO_2 : H_2O mass ratio of 9:100.

(2) Study on the content of gel agent

For the gel agent study, Gellan gum was selected, with concentrations chosen at the minimum (0.1 wt%) and maximum (0.3 wt%) typical usage levels. Gellan gum was first dissolved in deionized water, heated to 75°C, and stirred for 5 minutes to prepare solutions of the two concentrations. The solutions were then cooled to room temperature. Subsequently, dry-water powders containing different concentrations of Gellan gum were prepared by stirring at a ratio of SiO₂ to Gellan gum solution of 9:100 and a stirring speed of 24,000 r/min for 5 seconds, as shown in Fig. 5.



Fig. 5. Dry-water powders prepared with different concentrations of Gellan gum.

According to Fig. 5, adding 0.1% Gellan gum resulted in clumping of the powder particles, significant particle size variation, and poor stability. Adding 0.3% Gellan gum produced a mousse-like product that did not resemble dry-water powders; the overall product was thick and gel-like, indicating preparation failure. The variation in appearance of the dry-water powders with different Gellan gum contents is due to changes in the surface tension of the solution caused by the Gellan gum, which affects powder dispersion. At lower concentrations, Gellan gum has minimal impact on solution properties, resulting in successful formation of dry-water powders. At higher concentrations, the increased strength of the Gellan gum solution prevents breakup under the same shear force, leading to mousse-like products.

(3) Surfactant content study

To increase the Gellan gum content, three comparative experiments were conducted by adding different proportions (0.5%, 1%, 1.5%) of methyl hydrogen silicone oil to a sample containing 0.3% Gellan gum. The appearance of the products is shown in Fig. 6.

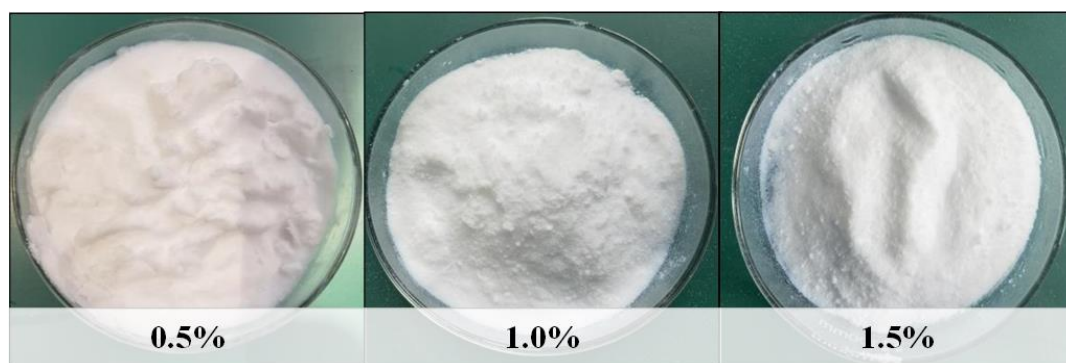


Fig. 6. Products of dry-water powder prepared with different concentrations of methyl hydrogen silicone oil.

Based on Figs. 5 and 6, the transition of the product from a mousse-like to a dry-water powder form was observed by adding different concentrations of methyl hydrogen silicone oil. When the content of methyl hydrogen silicone oil reached 1%, the product exhibited ideal dry-water powder characteristics, with excellent dispersibility and flowability. Therefore, this concentration is determined to be the basic preparation condition for the new dry-water powder.

2.4. Preparation of Novel Dry-water Powders

(1) Preparation of dry-water powders from aqueous solutions

Mg(OH)₂, aluminum hydroxide, and APP were each mixed with deionized water. Methyl hydrogen silicone oil and silica were added to the mixture, which was then stirred at 24,000 r/min for 5 seconds to produce the corresponding dry-water powders, as shown in Fig. 7.

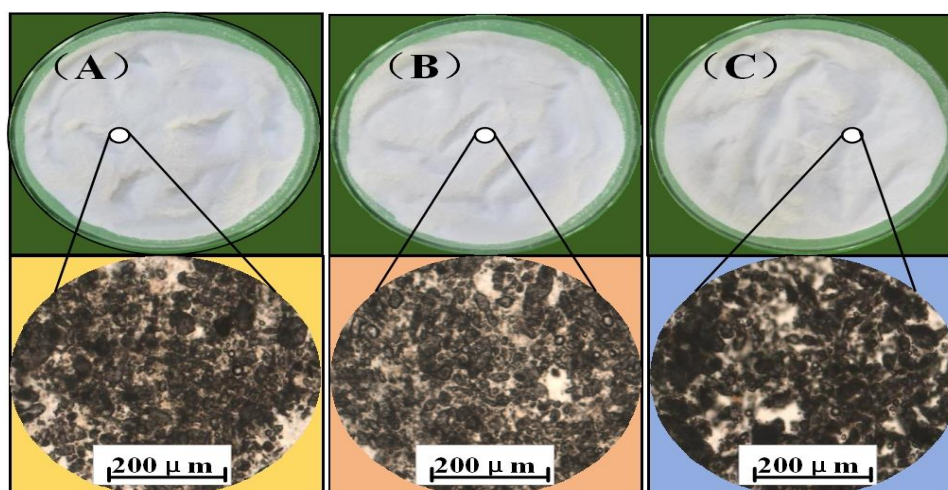


Fig. 7. Appearance and microscopic images of aqueous-type dry-water powders.

Fig. 7 demonstrates that the dry-water powders of Mg(OH)₂, Al(OH)₃, and APP exhibit ideal morphology, with no visible aqueous solutions or residual silica. The powders formed a stable core-shell structure, indicating a well-structured product with uniform particle size.

(2) Preparation of gel-type dry-water powders

Effective fire extinguishing agents were mixed with 100 g of deionized water. Gellan gum was added to three separate mixtures, which were then heated to 75°C and stirred at 300 r/min for 5 minutes. After cooling, hydrophobic silica and methyl hydrogen silicone oil were added and the mixture was stirred at 24,000 r/min for 5 seconds to obtain Mg(OH)₂ gel dry-water powder, Al(OH)₃ gel dry-water powder, and APP gel dry-water powder, as shown in Fig. 8.

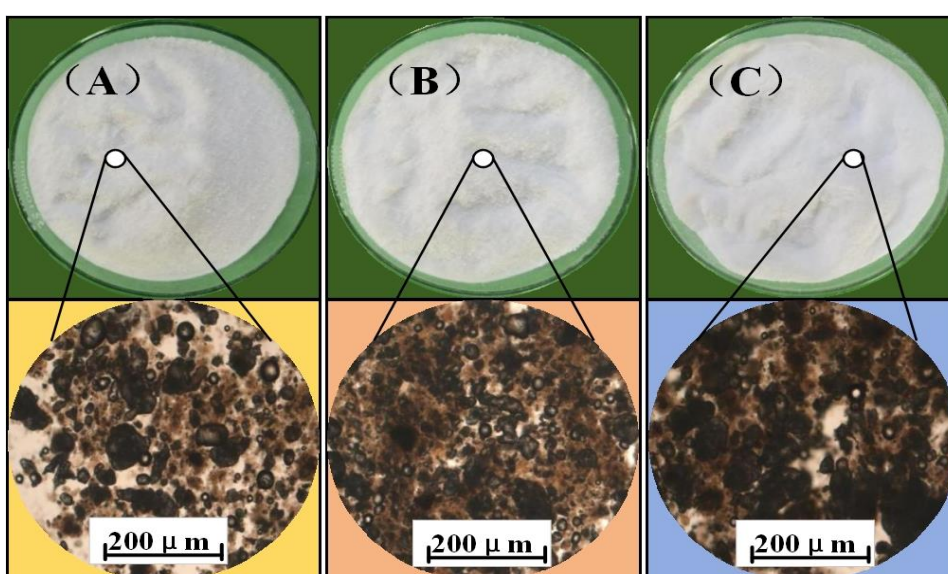


Fig. 8. Appearance and microscopic images of gel-type dry-water powders.

Fig. 8 shows that under optimized conditions, the $\text{Mg}(\text{OH})_2$, $\text{Al}(\text{OH})_3$, and APP gel dry-water powders exhibit surfaces free of visible aqueous solutions or residual silica, forming a stable core-shell structure. Compared to the aqueous-type powders, the gel-type dry-water powders have more regular particle shapes due to their unique gel network structure.

3. Characterization and analysis of the physicochemical properties of novel dry-water powders

To ensure that the newly developed dry-water powders meet the required physicochemical properties for effective fire extinguishment, performance characterization and comparison were conducted based on the dry powder fire extinguishing agent standard GB 4066-2017, powder physical property testing standards, and related research [34]. The key parameters assessed include flowability, bulk density, particle size distribution, and thermal stability.

3.1. Flowability testing

Powders with good flowability enhance the application and dispersion of extinguishing agents, reduce blockage issues, and improve spraying efficiency, thereby increasing fire extinguishing effectiveness. This can be quantified by measuring the powder flow rate and the angle of repose.

The procedure for flowability testing is depicted in Figure 9. This experiment employs a synchronous testing method to evaluate both the flow rate and the angle of repose of the dry-water powders. Initially, 100 grams of the powder sample were accurately weighed and placed in a funnel with a closed bottom. The funnel was then inverted and shaken four times to ensure uniform dispersion of the sample. Subsequently, the funnel was fixed above a glass plate, the bottom port was opened, and the time required for the powder to flow out was recorded. The angle of repose of the dry-water powders was calculated using Formula (1), based on the height and base radius of the conical pile formed on the glass plate.

The formula for calculating the angle of repose (Formula 1) is as follows:

$$\theta = \arctan \frac{h}{r}, \quad (1)$$

In the formula, θ is the angle of repose ($^\circ$), h is the actual height of the conical powder heap (cm), and r is the base radius of the conical powder (cm).

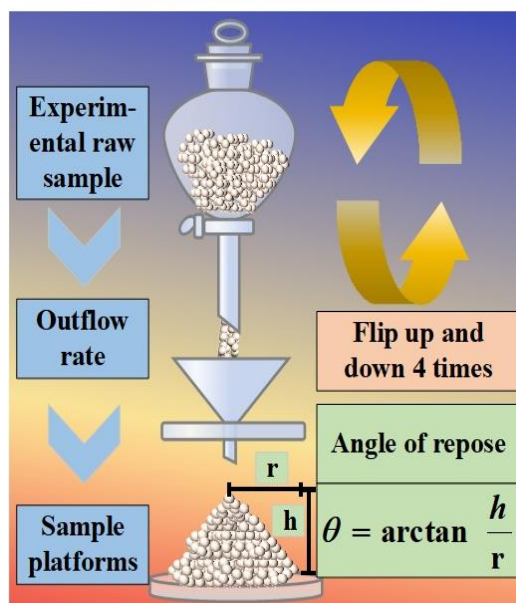


Fig. 9. Flowchart of the powder flowability experiment.

3.1.1. Flow Rate Experiment

According to the experimental procedure shown in Fig. 9, the outflow velocity of the powder was measured as shown in Fig. 10.

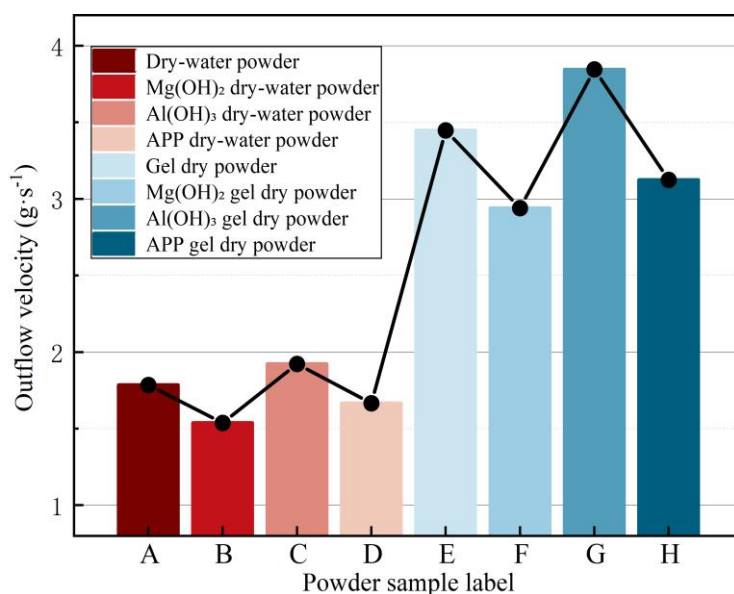


Fig. 10. Comparison of mean values of different powder outflow velocities.

As can be seen from Fig. 10, the gelling agent modification significantly enhances the flowability of dry aqueous powders. Among them, the $\text{Al}(\text{OH})_3$ gel dry-water powder exhibited the fastest flow rate at $3.846 \text{ g}\cdot\text{s}^{-1}$, followed by the gel dry-water powder at $3.460 \text{ g}\cdot\text{s}^{-1}$. Gelation modification optimized the particle morphology and distribution of the dry-water powders, reducing inter-particle friction and falling resistance, thereby enhancing the flowability of the powders.

3.1.2. Angle of repose experiment

According to the angle of repose equation, the results of the angle of repose test of the powder are shown in Fig. 11:

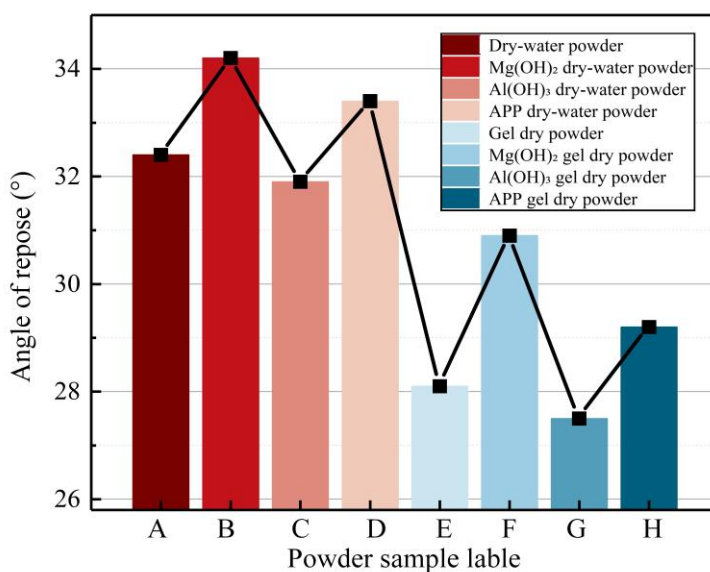


Fig. 11. Comparison of mean values of angle of repose for different powders.

According to Fig. 11, the repose angles of the eight types of dry-water powders are predominantly within the range of 27° to 35° . Among these, the repose angles of the gel-type dry-water powders are significantly smaller

than those of the liquid-type, ranging from 27° to 31°, which corroborates their faster flow rate and indicates that gel-type powders exhibit superior flowability. Further comparison of the water solution-type and gel-type dry-water powders, examining the effects of various effective fire extinguishing agents on flowability, reveals that the addition of $\text{Mg}(\text{OH})_2$ decreases the flowability of the dry-water powders, possibly due to increased surface roughness and internal aggregation; APP has a minimal effect on flowability but shows some promoting effect; whereas $\text{Al}(\text{OH})_3$ significantly enhances the flowability, attributed to the formation of hydrogen bonds and strong adsorption forces of aluminum ions in water, resulting in more uniform particles and a smoother surface.

In summary, the addition of gel agents significantly improves the flowability of the dry-water powders, while the inclusion of effective fire extinguishing components has a relatively minor overall impact on flowability, with $\text{Al}(\text{OH})_3$ demonstrating a significant positive enhancement effect on flowability.

3.2. Bulk Density Experiment

The bulk density of the dry-water powder, which is the ratio of the mass to the volume of the powder in its loose, natural state without compression, reflects the density value measured without external force or vibration. Generally, materials with a higher bulk density can accommodate more powder in the same volume. The experiment involves adjusting the height of the powder tray to ensure it contacts the bottom of the funnel. A 30 mL sample of dry-water powder is allowed to naturally accumulate in the tray via the funnel. Record and repeat the experiment as shown in Fig. 9 and take the average value, substitute into the formula to calculate the bulk density.

The calculation formula is as follows:

$$D_0 = \frac{M_0}{V_0}, \quad (2)$$

In the formula, D_0 represents the bulk density, M_0 is the mass (g/cm^3), and V_0 is the volume (cm^3).

The bulk density of the new dry-water powder was measured using the JL-A3 powder characteristics tester. The results were analyzed for error bars and visually compared to obtain the bulk density comparison of different powders, as shown in Fig. 12.

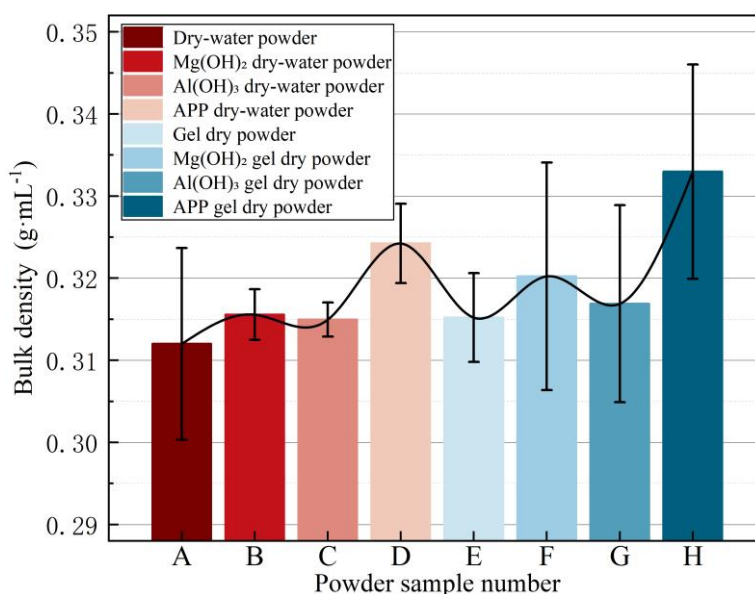


Fig. 12. Comparison of bulk densities of different powders.

From Fig. 12:

(1) The bulk density of the new dry-water powders ranges from 0.312 to 0.333 g/mL, which is significantly lower than the 0.82 g/mL of conventional dry powder fire extinguishers. This is attributed to their core-shell structure, where the large voids and porous structure result in a fluffy powder, increasing the volume and decreasing the bulk density. The addition of gel agents enhances the bulk density, as gelation increases the internal mechanical strength, making the powder more compact. Gel-type dry-water powders exhibit an increased bulk

density compared to the original, indicating a higher capacity for fire extinguishing material.

(2) Modification with $\text{Mg}(\text{OH})_2$, $\text{Al}(\text{OH})_3$, and APP results in an increase in the bulk density of dry-water powders. This is due to the increase in effective fire extinguishing components, which enhances the internal solution quality, density, and overall density. Among these, APP has a significant impact on bulk density, increasing the bulk density of dry-water powders by 0.012 g/mL and gel-type dry-water powders by 0.018 g/mL, while $\text{Mg}(\text{OH})_2$ has a lesser effect and $\text{Al}(\text{OH})_3$ a minor one. The high hygroscopicity of $\text{Al}(\text{OH})_3$ results in smaller particles of the dry-water powder, but increases the bulk density, indicating a higher content and efficiency of fire extinguishing material.

In summary, both gel agents and effective fire extinguishing component modifications effectively enhance the bulk density of dry-water powders, with APP showing particularly significant improvement, thus providing an effective pathway for optimizing fire extinguishing performance.

3.3. Particle Size Distribution Experiment

The particle size of dry-water powder is primarily determined using laser analysis technology, which assesses particle size through the degree of light deflection [35]. Larger particles are associated with less light deflection, whereas smaller particles, owing to their increased specific surface area, demonstrate enhanced fire extinguishing efficacy.

The experiment utilizes a reagent dispersion method, employing ethanol as the dispersant. The laser particle size analyzer is preheated for 15 minutes, and its parameters are adjusted according to the background light energy distribution map. Anhydrous ethanol and the dry-water powder sample are introduced into the sample chamber, stirred for 5 minutes, and subjected to ultrasonic treatment. Subsequently, testing began, and the detailed particle size distribution (PSD) is shown in Figs. 13 to 20.

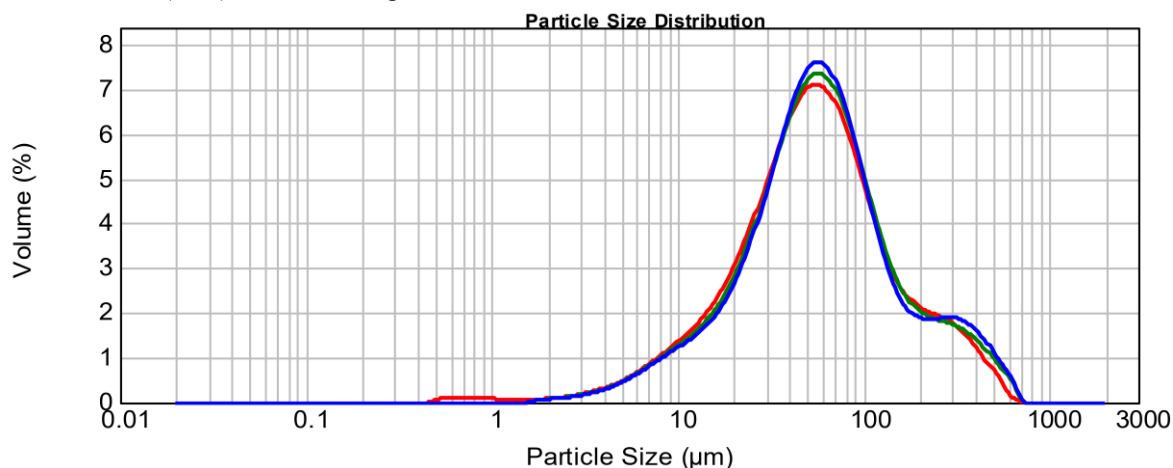


Fig. 13. PSD of dry-water.

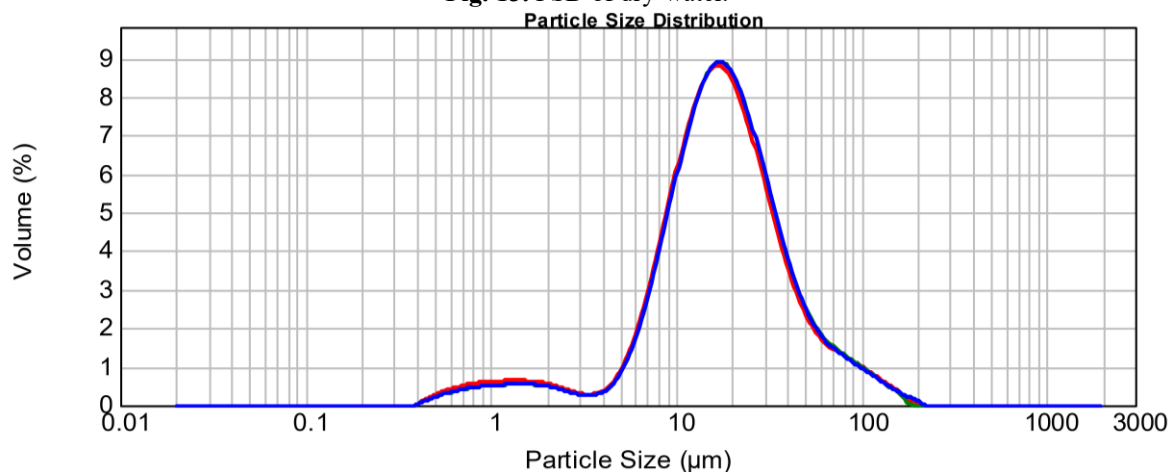


Fig. 14. PSD of $\text{Mg}(\text{OH})_2$ dry-water powder.

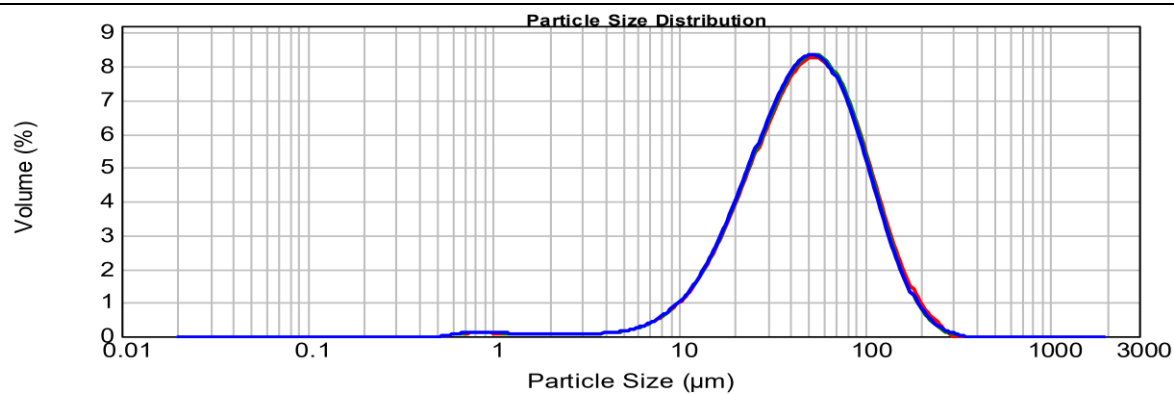


Fig. 15. PSD of $\text{Al}(\text{OH})_3$ dry-water powder.

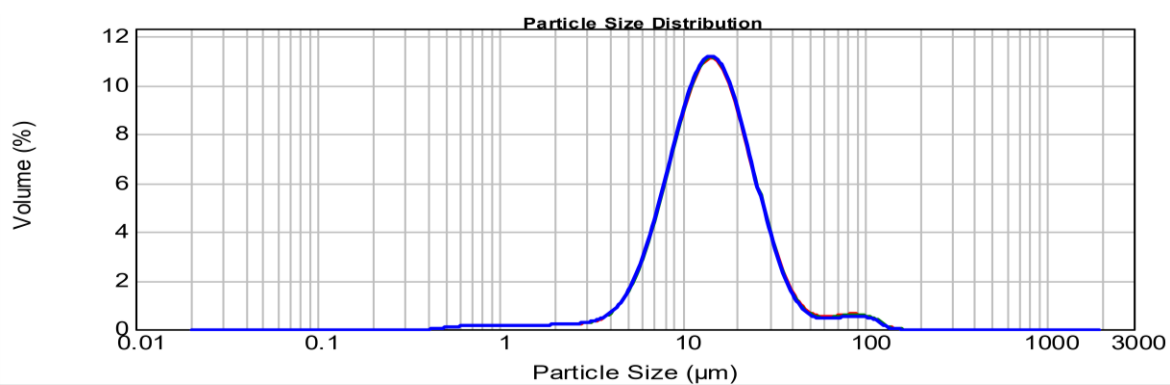


Fig. 16. PSD of APP dry-water powder.

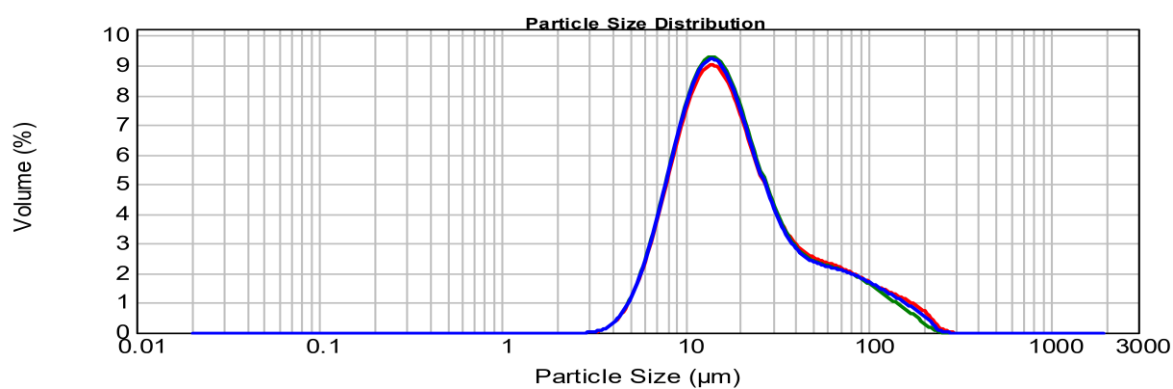


Fig. 17. PSD of gel dry-water powder.

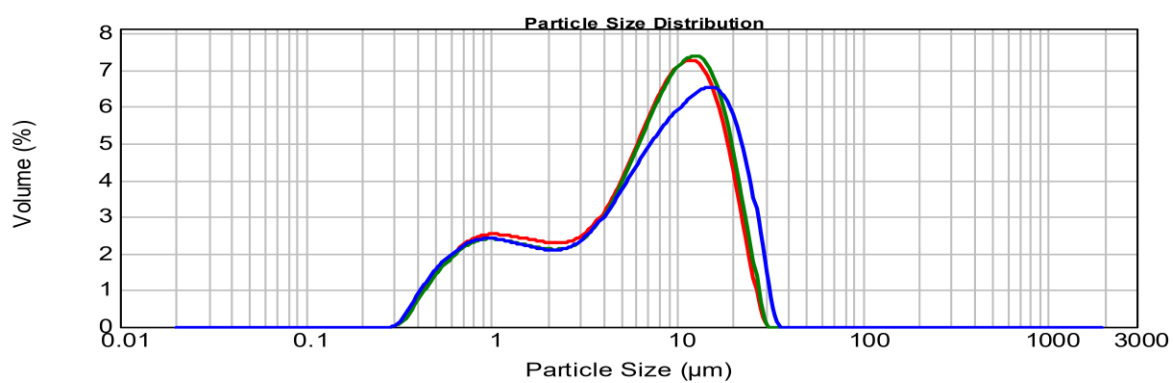


Fig. 18. PSD of $\text{Mg}(\text{OH})_2$ gel dry-water powder.

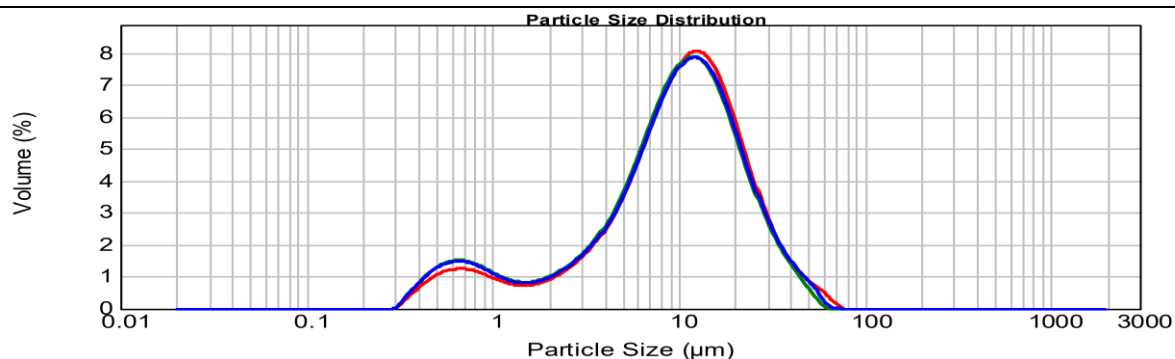


Fig. 19. PSD of $\text{Al}(\text{OH})_3$ gel dry-water powder.

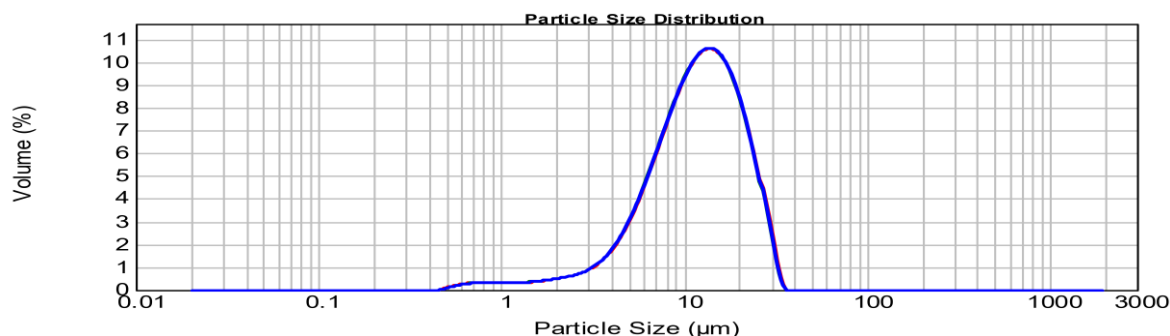


Fig. 20. PSD of APP gel dry-water powder.

Under identical experimental conditions, laser particle size analysis was conducted on the novel dry-water powders. The results of the particle size analysis for eight types of dry-water powders, obtained from the laser particle size analyzer report (d10, d50, d90), are presented. The particle size distribution trends for each powder, based on the mean particle size, are illustrated in Fig. 21. The d90 value indicates that 90% of the particles have a size smaller than this value, d50 denotes that 50% of the particles have a size smaller than this value, and d10 signifies that 10% of the particles have a size smaller than this value.

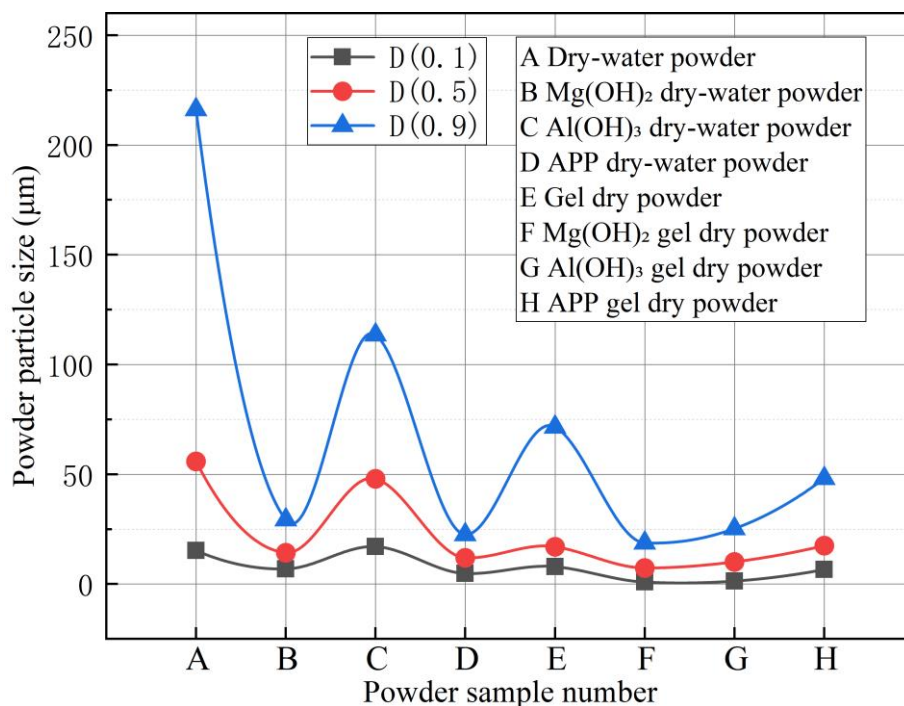


Fig. 21. Comparison of particle size distribution trends for different dry-water powders at three sizes.

Figs 13 to 21 reveal that the particle sizes of the novel dry-water powders are predominantly below 250 μm and exhibit a normal distribution, indicating high particle size uniformity and conforming to the typical particle size distribution characteristics of dry-water powders. Further comparison between gel-type and aqueous solution-type dry-water powders reveals that the gel-type powders have smaller particle sizes. This is attributed to the addition of Gellan gum, which enhances the core material's structural strength, making it easier to form stable, cohesive small droplets during the shearing process.

A horizontal comparison of the effects of effective fire-extinguishing components on the particle size of dry-water powders shows that with the addition of these components, the particle size of the powders decreases, indicating more uniform particles and more ideal morphology. This is mainly due to the effective fire-extinguishing components reducing the surface tension of the core material of the dry-water powders, increasing the difficulty of forming a core-shell network structure. During preparation, compared to pure water dry-water powders, only smaller droplets of the core material can be coated with silica. It is noteworthy that the $\text{Mg}(\text{OH})_2$ gel dry-water powder exhibits the smallest overall particle size.

In summary, the particle size of gel-type dry-water powders is smaller than that of aqueous solution-type dry-water powders, and the addition of effective fire-extinguishing components results in varying degrees of reduction in particle size.

3.4. Thermal stability experiment

Thermogravimetric analysis (TGA) is a critical method for assessing the thermal stability of dry-water powders. It involves monitoring the mass changes of the powders during heating to investigate their thermal stability, moisture content, and volatiles. The dry-water powder samples are placed in the test chamber, with nitrogen (N_2) used as the protective gas. The thermogravimetric analyzer is set to a heating rate of $20^\circ\text{C}/\text{min}$ over a temperature range of 20 to 800°C . The analyzer is then started, and the mass changes of the samples are recorded during the temperature increase. Thermogravimetric curves are plotted based on the experimental results to analyze the weight loss process, including possible moisture evaporation, chemical reactions, and combustion. The powder thermogravimetric percentage change is shown in Fig. 22.

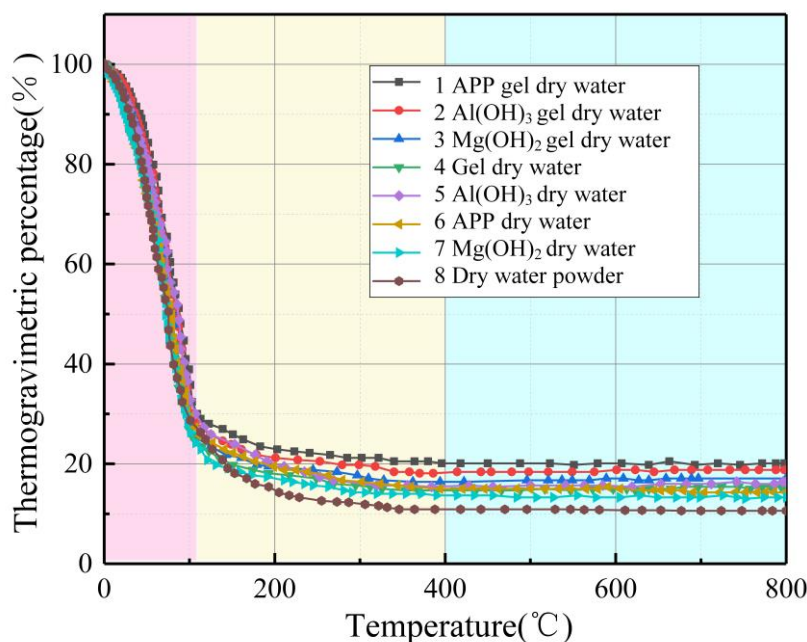


Fig. 22. Thermogravimetric percentage variation of different dry-water powders.

The thermogravimetric curves of the eight types of dry-water powders can be divided into three stages: 20– 110°C , where surface water and some bound water desorb, causing a decrease in sample weight and a downward curve; 110 – 400°C , where bound water desorbs and effective fire-extinguishing components react or decompose, resulting in a downward trend; and 400 – 800°C , entering the stable pyrolysis stage, indicating a slowdown or near cessation of weight loss in this temperature range. Comparing the effects of modifiers on the thermogravimetric

analysis, it is evident that after modification with effective fire-extinguishing components and gelation, the thermal weight loss of the dry-water powders is significantly reduced. This indicates that the modified dry-water powders can retain more fire-extinguishing components when exposed directly to the fire source. The residual amounts, from highest to lowest, are: 1>2>3>4>5>6>7>8.

In summary, the thermogravimetric curves of the dry-water powders exhibit similar overall trends, with the gel-type powders demonstrating higher thermal stability compared to the aqueous-type powders. Among the effective fire-extinguishing components, APP significantly enhances the thermal stability of the dry-water powders.

4. Study on the fire-extinguishing performance of novel dry-water powders

Based on the characterization of the physicochemical properties of the novel dry-water powders, gelation significantly enhanced these properties, while the addition of the three active fire-extinguishing components had minimal impact. Therefore, gelled dry-water powders, both alone and in combination with $\text{Mg}(\text{OH})_2$, $\text{Al}(\text{OH})_3$, and APP, were selected as new fire-extinguishing agents, with the gelled dry-water powder serving as the control group.

4.1. Small-scale dry-water powder fire-extinguishing system and experimental procedure

Based on the characteristics of insulation material fires and relevant studies, including GB/T 20284-2006 "Single Burning Item Test for Building Materials or Products" [36-38], this paper designs an open-air small-scale powder spraying fire-extinguishing experimental system. The experimental conditions are controlled at a temperature of $24 \pm 2^\circ\text{C}$, atmospheric pressure of $101.13 \pm 3 \text{ kPa}$, relative humidity of $60 \pm 5\%$, and wind force below level 2. The experimental system includes modules for combustion, data acquisition, and powder spraying, and employs the controlled variable method for testing. The schematic diagram of the experimental procedure is shown in Fig. 23.

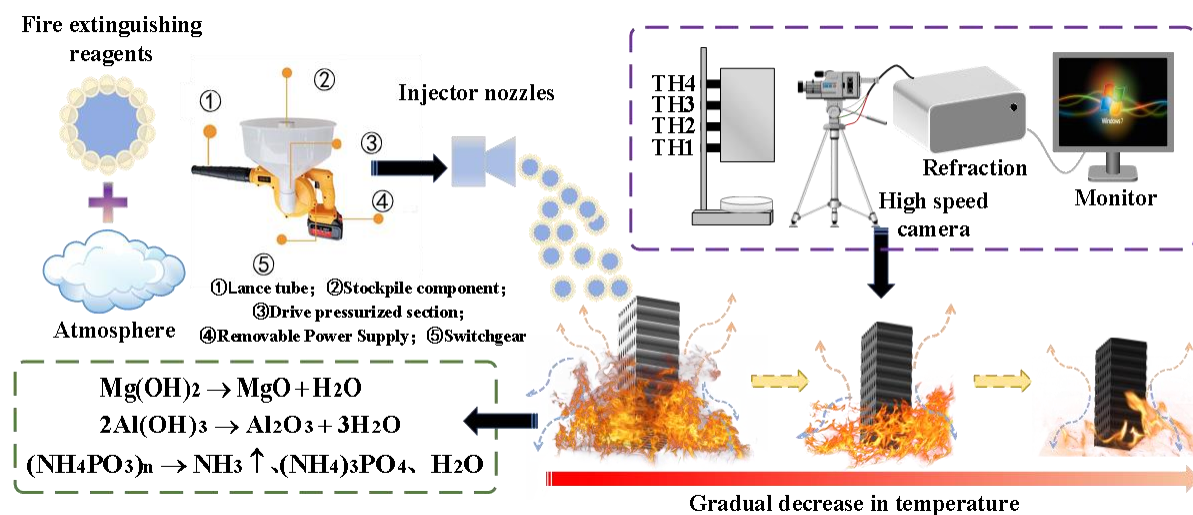


Fig. 23. Schematic Diagram of the Small-Scale Dry-Water Powder Fire-Extinguishing System Process.

Before the experiment, the heat release rate of the fire source was determined using a small oil pan (with n-heptane as fuel, 50 mL per test) and thermocouple placement (TH1 to TH4 from bottom to top, spaced 5 cm apart along the central axis of the oil pan). The temperature variation data at which the fire self-extinguishes were also recorded to provide fundamental parameters for the fire-extinguishing experiment.

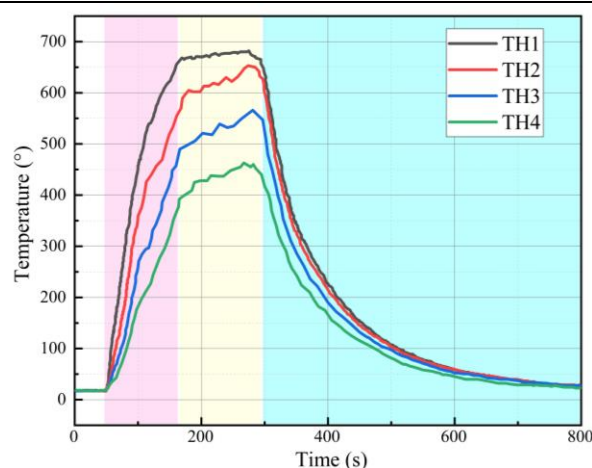


Fig. 24. Temperature variation graph of n-heptane during self-extinguishment.

Fig. 24 illustrates the self-extinguishment process of n-heptane, encompassing three stages: ignition growth, stable combustion, and decay. The heat release rate (HRR) of n-heptane can be calculated using Equation 3:

$$HRR = \alpha \times m \times \Delta H, \quad (3)$$

In the equation, HRR is the heat release rate, kW; α is the combustion efficiency factor, usually taken as 0.3~0.9; m is the mass loss rate of the fuel, kg/s; and ΔH is the combustion calorific value of the fuel, kJ/kg.

Based on Fig. 24, it can be observed that the combustion of n-heptane is relatively complete. In this study, the combustion efficiency factor is set at 0.9. The mass difference of n-heptane before and after combustion is 32 g, with an ignition rise phase time of 115 s. The calculated mass loss rate is 2.783×10^{-4} kg/s, and the heat of combustion is 44.6×10^3 kJ/kg, leading to a heat release rate of 11.17 kW for n-heptane. Consequently, all combustion tests conducted in this study are performed under a heat release rate condition of 11.17 kW.

4.2. Study on the injection time and fire extinguishing performance of thermal insulation material fire extinguishing agents

This study is based on a fixed fire model, where an 11.17 kW fire source is ignited beneath a $30 \times 20 \times 5$ cm³ rectangular combustible material, to investigate the temperature changes and mass loss characteristics of various insulation materials, including EPS, XPS, and PU, during combustion. By measuring temperature changes during combustion and the mass of residual materials post-combustion, the optimal powder spraying time for these materials is determined.

(1) Complete combustion of EPS

Fig. 25 shows that during EPS combustion, the flame temperature rises significantly between 30 and 120 seconds, with the TH1 thermocouple recording a peak temperature of 281°C. This phase includes two main phenomena: volatilization and plastic combustion. During the volatilization phase, volatile substances in EPS are released and combust, leading to a temperature increase. Following this, the plastic combustion phase involves the combustion of polystyrene molecular chains, releasing heat to sustain the flame and generate smoke. After 120 seconds, the temperature gradually stabilizes and decreases, returning to room temperature by 1000 seconds, with a residual mass of 13 g.

Rapidly extinguishing the fire source at the onset of a fire involving insulation materials can prevent the fire from spreading and reduce damage. Based on the EPS combustion temperature curve, a powder spraying time of 25 seconds is selected when the temperature reaches 100°C, and different extinguishing agents are tested to evaluate their performance.

(2) Complete combustion of XPS

Fig. 26 indicates that within 30 to 90 seconds, the flame temperature rises significantly, with the TH1 thermocouple recording a temperature as high as 333°C, indicating that XPS releases more heat and carbon residues compared to EPS. The rapid combustion of XPS results in early carbonization and droplet formation,

attributed to the high-temperature smoke concentration produced. Subsequently, XPS burns steadily between 90 and 350 seconds, after which the temperature gradually decreases to ambient levels. The residual mass after combustion is 24 g. Based on the combustion temperature curve, a powder spraying time of 10 seconds is chosen when the temperature reaches 100°C.

(3) Complete combustion of PU

Fig. 27 demonstrates that, compared to EPS and XPS, PU exhibits a significantly lower rate of temperature rise due to its stable material properties and high density. During combustion, PU's flame temperature rises rapidly between 30 and 320 seconds, with the TH1 thermocouple recording a maximum temperature of 168°C, accompanied by black smoke. Subsequently, PU's temperature begins to stabilize and decline. Notably, in the later stages of combustion, temperatures recorded by TH2, TH3, and TH4 are higher than those recorded by TH1, indicating that PU maintains structural stability and its insulation performance is not fully compromised in the small-scale model. The residual mass post-experiment is 132 g. Based on the PU combustion temperature curve, a powder spraying time of 180 seconds is selected when the temperature reaches 100°C.

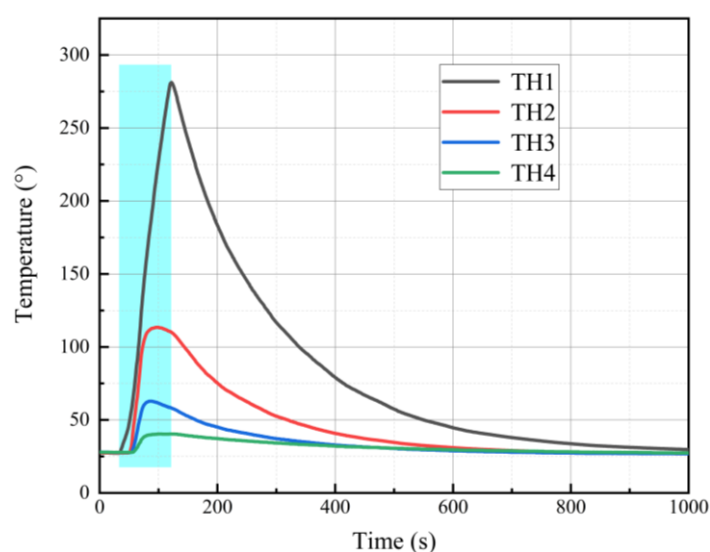


Fig. 25. Temperature changes during complete combustion of EPS.

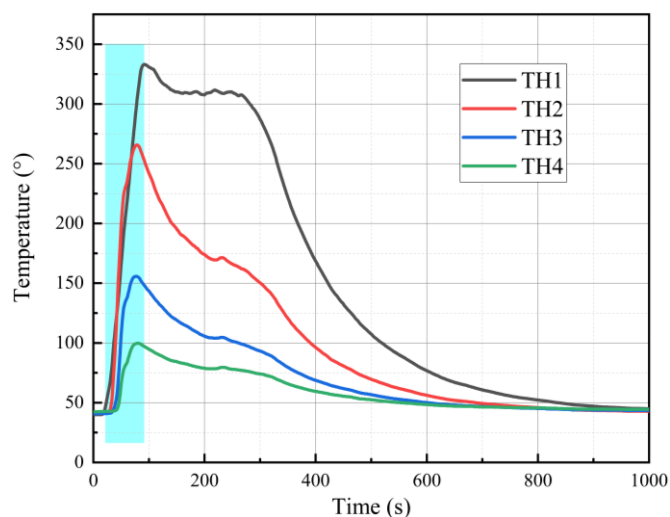


Fig. 26. Temperature changes during complete combustion of XPS.

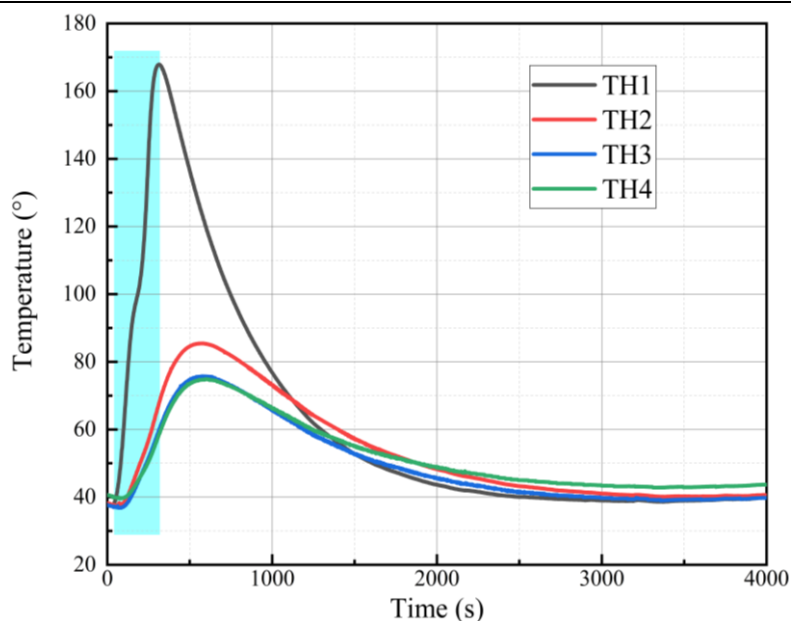


Fig. 27. Temperature changes during complete combustion of XPS.

4.3. Characterization and analysis of the fire extinguishing performance of novel dry-water powders

This study evaluates the fire extinguishing performance of dry powders on three types of insulation materials: EPS, XPS, and PU, through flame suppression experiments at specific discharge times. Based on temperature change graphs during combustion, the optimal discharge time was determined. Since the extinguishing agents were applied before the temperature of the insulation material increased significantly, resulting in similar temperature change trends across materials, this study uses the cooling rate of the insulation material within 30 seconds after powder discharge as a representative indicator of temperature change.

(1) Study on flame suppression for EPS

Based on the temperature change results from thermocouples of EPS after applying different extinguishing agents for 30 seconds, the cooling rates of EPS within 30 seconds after discharge can be calculated using Equation (4), resulting in the EPS cooling rate graph as shown in Fig. 28.

$$\Delta T = \frac{T_1 - T_2}{t}, \quad (4)$$

In the equation, ΔT is the rate of temperature change, °C/s; T_1 is the initial temperature, °C; T_2 is the termination temperature, °C; t is the temperature change time, s.

As shown in Fig. 28, the cooling rate of EPS decreases as the distance from the fire source increases. Among the extinguishing agents, the cooling rate of APP dry powder is the highest. Comparing the cooling rates of different extinguishing agents, dry powder agents generally exhibit higher cooling rates than ABC dry powder extinguishers. $\text{Mg}(\text{OH})_2$, $\text{Al}(\text{OH})_3$, and APP gel dry powders effectively suppress the fire during EPS combustion by absorbing heat, releasing hydroxyl ions, and promoting carbonization, thereby slowing the spread of the fire. In summary, among the five extinguishing agents provided in this study, APP gel dry powder performs the best for EPS fires, followed by $\text{Mg}(\text{OH})_2$ gel dry powder and $\text{Al}(\text{OH})_3$ gel dry powder.

(2) XPS flame suppression study

Fig. 29 indicates that the flame temperature rises significantly within 30-90 seconds, with a peak temperature of 333 °C recorded by the TH1 thermocouple, demonstrating that XPS releases more heat and carbon residues than EPS during combustion. The rapid burning of XPS results in early carbonization and dripping from the upper part, due to the concentrated high-temperature smoke generated. Subsequently, XPS exhibits stable burning from 90 to 350 seconds, after which the temperature gradually decreases to ambient temperature. The residue after combustion weighs 24 g. Based on the combustion temperature curve, a spraying time of 10 seconds was selected when the temperature reaches 100°C.

(3) PU flame suppression study

According to Fig. 30, APP gel dry powder and $\text{Al}(\text{OH})_3$ gel dry powder demonstrated the best extinguishing performance, increasing the cooling rates by 0.113 and 0.244 $^{\circ}\text{C}/\text{s}$, respectively. This is primarily attributed to the effective extinguishing components in the dry powders during PU combustion. The water molecules and hydroxyl ions (OH^-) released by $\text{Al}(\text{OH})_3$ capture free radicals generated during PU combustion, while APP generates phosphoric acid and forms a stable foam carbon layer, which creates a lower temperature and stable foam carbon layer that interrupts the combustion reaction chain of PU.

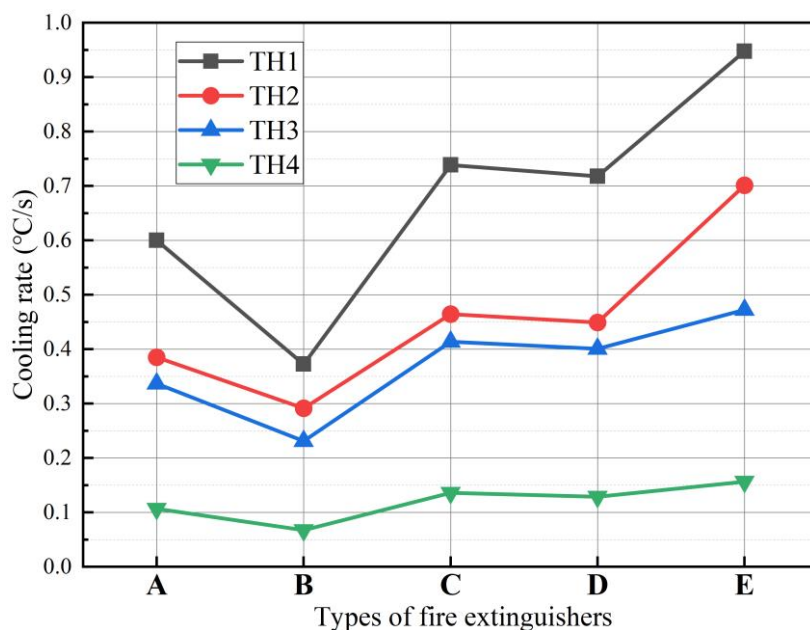


Fig. 28. Plot of cooling rate of EPS in 30s after injection of different extinguishing agents: A: Gel dry powder; B: ABC dry powder; C: $\text{Mg}(\text{OH})_2$ gel dry powder; D: $\text{Al}(\text{OH})_3$ gel dry powder; E: APP gel dry powder. Same hereafter.

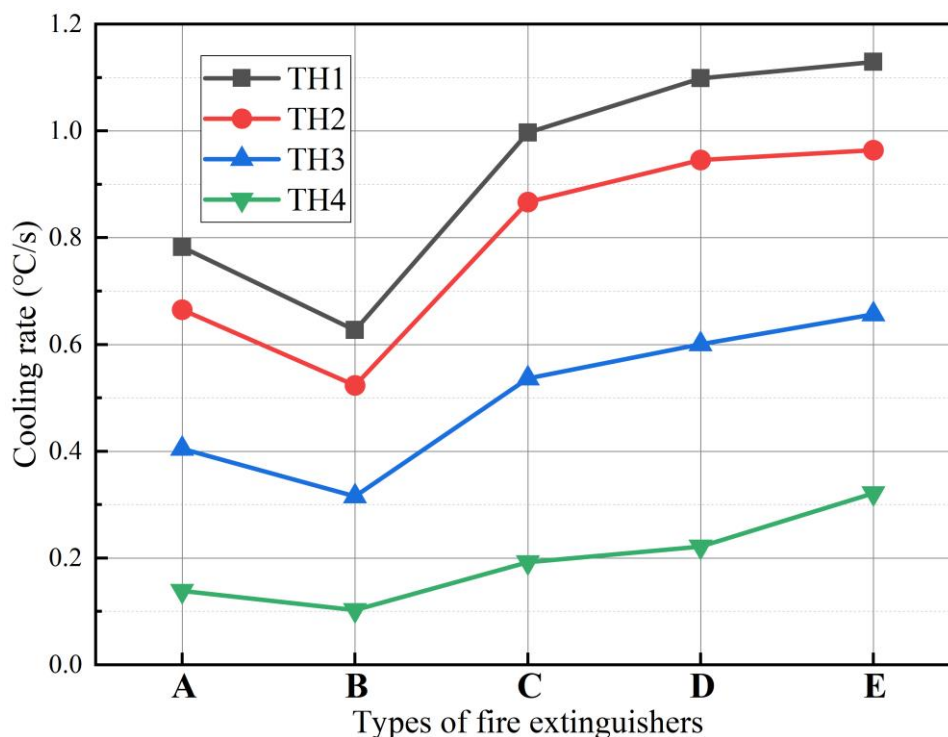


Fig. 29. Plot of cooling rate of XPS in 30s after injection of different extinguishing agents.

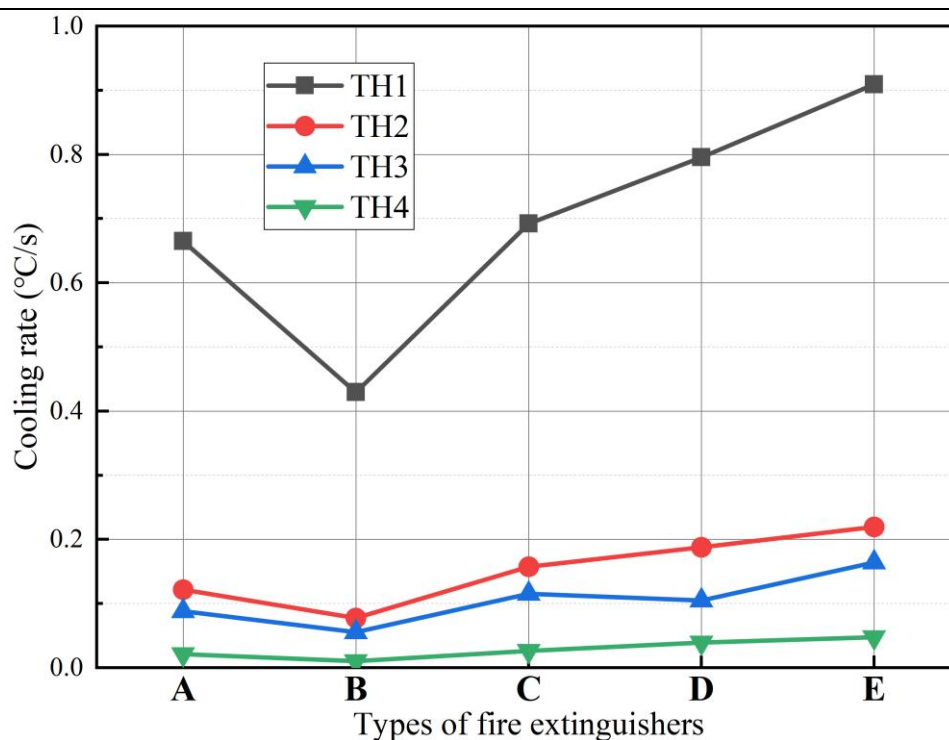


Fig. 30. Plot of cooling rate of PU in 30s after injection of different extinguishing agents.

In summary, the novel dry powder exhibits cooling, smothering, and chemical suppression effects in suppressing flames from thermal insulation materials, demonstrating superior fire-extinguishing performance compared to ABC dry powder. Among the tested agents, APP gel dry powder and $\text{Al}(\text{OH})_3$ gel dry powder show particularly promising fire-extinguishing efficacy, indicating significant potential for application.

5. Conclusion

- (1) By optimizing the stirring speed (24,000 r/min), stirring time (5 s), and material ratios (SiO_2 mass ratio of 9:100), and incorporating 1% methyl hydrogen silicone oil along with fire-extinguishing agents such as $\text{Mg}(\text{OH})_2$, $\text{Al}(\text{OH})_3$, and APP, eight types of dry powders were prepared: dry powder, $\text{Mg}(\text{OH})_2$ dry powder, $\text{Al}(\text{OH})_3$ dry powder, APP dry powder, gel dry powder, $\text{Mg}(\text{OH})_2$ gel dry powder, $\text{Al}(\text{OH})_3$ gel dry powder, and APP gel dry powder.
- (2) The spray performance of the newly modified core-shell gel dry powders has been significantly enhanced. The gelation modification method exhibits a stronger surface tension reduction effect, resulting in superior flow properties, with the $\text{Al}(\text{OH})_3$ gel dry powder showing an outflow rate of $3.846 \text{ g} \cdot \text{s}^{-1}$ and a repose angle of 27.5° . The bulk density of the new dry powders is generally lower, with the APP gel dry powder having the highest bulk density of $0.333 \text{ g} \cdot \text{mL}^{-1}$. Particle size analysis reveals that the $\text{Mg}(\text{OH})_2$ gel dry powder has the smallest particle size, with d_{10} of $15.323 \text{ } \mu\text{m}$, d_{50} of $55.922 \text{ } \mu\text{m}$, and d_{90} of $216.172 \text{ } \mu\text{m}$. Thermal weight loss variations are similar among different new dry powders.
- (3) The novel gel dry powders demonstrate effective fire-extinguishing performance against fires involving three types of thermal insulation materials. The time required for these materials to reach 100°C is 10 s, 25 s, and 180 s respectively, with these times serving as reference points for powder spraying. In the fire-extinguishing effectiveness tests, dry powder types generally outperform ABC dry powder. APP gel dry powder exhibits excellent performance in suppressing EPS and XPS flames, while $\text{Al}(\text{OH})_3$ gel dry powder also shows good fire-extinguishing efficacy against EPS and PU flames.

Declaration of Competing Interest

The authors declare that they have no known competing financial interests or personal relationships that could have appeared to influence the work reported in this paper.

Data statement

Data will be made available upon reasonable request.

Acknowledgments

This work was supported by the National Natural Science Foundation of China [grant number 52074213]; Key R&D Programme Key Special Projects of China [grant number 2018JMC0808201]; and Shaanxi Provincial Natural Science Foundation Basic Research Program Project [grant numbers 2018JM5009, 2018JQ5080]; and Shaanxi Science and Technology Association Young Talents Lifting Project [grant number 20240205]. We are grateful for the support of the Xi'an Research Center of National Mine Rescue.

References

- [1] Y. Ha, J. Jeon, Thermogravimetric analysis and pyrolysis characterization of expanded–polystyrene and polyurethane–foam insulation materials, *Case Studies in Thermal Engineering*. 2024 Feb 1;54:104002. <https://doi.org/10.1016/j.csite.2024.104002>.
- [2] Y. Tan, W. Chen, Y. Fang, M. Cheng, S. Wang, Investigation of novel expandable polystyrene/alumina aerogel composite thermal insulation material, *Energy*. 2023 Dec 1;284:129238. <https://doi.org/10.1016/j.energy.2023.129238>.
- [3] J. Zhao, F. Xue, Y. Fu, S. Lu, H. Zhang, Insights into the particle diameter and base chosen for dry powder fire extinguishing agents, *Fire and Materials*. 2023 Oct;47(6):774-83. <https://doi.org/10.1002/fam.3117>.
- [4] H. Li, L. Feng, D. Du, X. Guo, M. Hua, X. Pan, Fire suppression performance of a new type of composite superfine dry powder, *Fire and Materials*. 2019 Dec;43(8):905-16. <https://doi.org/10.1002/fam.2750>.
- [5] Q. Dong, J. Qi, S. Lu, L. Shi, Synergistic effects of typical clean gaseous fire-extinguishing agents, *Fire Safety Journal*, 2024 Jun 18:104206. <https://doi.org/10.1016/j.firesaf.2024.104206>.
- [6] Y. Dong, C.Y. Zhao, X.Z. Lv, T.W. Zhang, C.W. Zhang, Application techniques for micro capsules on energy security: A case study on Class B fire, *InIOP Conference Series: Earth and Environmental Science* 2021 Jun 1 (Vol. 766, No. 1, p. 012049). IOP Publishing. <https://doi.org/10.1088/1755-1315/766/1/012049>.
- [7] Q. Wang, F. Wang, C. Li, Z. Li, R. Li, Fire extinguishing performance and mechanism for several typical dry-water extinguishing agents, *RSC advances*. 2021;11(17):9827-36. <https://doi.org/10.1039/D1RA00253H>.
- [8] I.A. Rahman, P. Vejayakumaran, C.S. Sipaut, J. Ismail, C.K. Chee, Effect of the drying techniques on the morphology of silica nanoparticles synthesized via sol–gel process, *Ceram. Int.* 34 (2008) 2059–2066. <https://doi.org/10.1016/j.ceramint.2007.08.014>.
- [9] Y. Wang, G. Zhu, G. Chai, Y. Zhou, C. Chen, W. Zhang, Experimental study on the effect of release pressure on the extinguishing efficiency of dry-water, *Case Studies in Thermal Engineering*. 2021 Aug 1;26:101177. <https://doi.org/10.1016/j.csite.2021.101177>.
- [10] Q. Wang, B. Peng, Z. Luo, H. Wen, W. Gao, C.M. Shu, R. Min, Y. Sheng, X. Jiang, Gas explosion suppression performance of modified gel-type dry-waters, *Powder Technology*. 2023 Apr 15;420:118378. <https://doi.org/10.1016/j.powtec.2023.118378>.
- [11] L. Ai, G.C. Maitland, K. Hellgardt, Formation and phase equilibria of gas hydrates confined in hydrophobic nanoparticles, *Chemical Engineering Science*. 2024 Jun 17:120392. <https://doi.org/10.1016/j.ces.2024.120392>.
- [12] Y. Wei, N. Maeda, Dry-water as a Promoter for Gas Hydrate Formation: A Review, *Molecules*. 2023 Apr 26;28(9):3731. <https://doi.org/10.3390/molecules28093731>.
- [13] F. Zhang, X. Wang, B. Wang, X. Lou, W. Lipiński, Experimental and numerical analysis of CO₂ and CH₄ hydrate formation kinetics in microparticles: A comparative study based on shrinking core model, *Chemical Engineering Journal*. 2022 Oct 15;446:137247. <https://doi.org/10.1016/j.cej.2022.137247>.
- [14] L.S. Podenko, A.O. Drachuk, N.S. Molokitina, A.N. Nesterov, Multiple methane hydrate formation in powder poly (vinyl alcohol) cryogel for natural gas storage and transportation, *Journal of natural gas science and engineering*. 2021 Apr 1;88:103811. <https://doi.org/10.1016/j.jngse.2021.103811>.
- [15] F. Golkhou, A. Haghtalab, Kinetic and thermodynamic study of CO₂ storage in reversible gellan gum supported dry-water clathrates, *Journal of the Taiwan Institute of Chemical Engineers*. 2020 Oct 1;115:79-95. <https://doi.org/10.1016/j.jtice.2020.09.034>.

-
- [16] J. Yoo, J.H. Kim, D. Kim, Fire extinguishing device using nanoenergetic materials and dry-water, *Powder Technology*. 2024 Jul 1;443:119935. <https://doi.org/10.1016/j.powtec.2024.119935>.
- [17] W. Guo, G. Zhu, B. Yao, F. Chen, X. Xu, Study on the fire extinguishing mechanism of small size wood crib based on small sand-throwing equipment, *Case Stud. Therm. Eng.* 25 (2021) 100942. <https://doi.org/10.1016/j.csite.2021.100942>.
- [18] X. Li, K. Du, Y. Zhu, Z. Zhou, X. Zhou, Dry-water: Toward an ideal extinguishant for lithium-ion battery fire, *Journal of Energy Storage*. 2024 Mar 1;80:110204. <https://doi.org/10.1016/j.est.2023.110204>.
- [19] E.V. Saenko, Y. Huo, A.Sh. Shamsutdinov, N.B. Kondrashova, I.V. Valtsifer, V.A. Valtsifer, Mesoporous Hydrophobic Silica Nanoparticles as Flow-Enhancing Additives for Fire and Explosion Suppression Formulations, *ACS Appl Nano Mater* 2020;3:2221–33. <https://doi.org/10.1021/acsanm.9b02309>.
- [20] H. Liu, T. Zhang, C. Zhang, L. Xiao, Q. Liang, Application of a novel a core-shell microstructured nanocomposites as a fire extinguishant using seawater, *E3S Web Conf.* 237 (2021) 01009. <https://doi.org/10.1051/e3sconf/202123701009>.
- [21] L. Zhang, Y. Ji, D. Kuai, S. Shu, Preparation and inhibition performance of dry-water materials for preventing spontaneous combustion of coal, *Fuel*. 2023 Nov 15;352:129131. <https://doi.org/10.1016/j.fuel.2023.129131>.
- [22] C. Xue, H. Jiang, C. Zhu, W. Gao, Dry-water consisting of nano SiO₂ modified by fluorinated surfactant: Applied to AlH₃ explosion suppression, *Powder Technology*. 2024 Jan 15;433:119246. <https://doi.org/10.1016/j.powtec.2023.119246>.
- [23] T. Wang, Z. Yang, P. Yang, W. Yi, J. Deng, Z. Luo, Y. Sheng, F. Meng, Z. Dong, The deflagration suppression effect of ammonium salt-modified dry-water on methane-air mixtures: An experimental investigation, *Powder Technology*. 2024 Feb 1;434:119313. <https://doi.org/10.1016/j.powtec.2023.119313>.
- [24] J. Cheng, Z. Ma, Q. Fu, D. Ran, M. Borowski, Z. **, Eco-friendly extinguishing three-phase-gel foam with novel particle-gel crosslinking enhancing stabilization and fire extinguishing, *Powder Technology*. 2024 Jul 31:120134. <https://doi.org/10.1016/j.powtec.2024.120134>.
- [25] S. Tian, B. Qin, D. Ma, Q. Zhou, Z. Lou, Suppressive effects of alkali metal salt modified dry-water material on methane-air explosion, *Energy*. 2023 Dec 15;285:129547. <https://doi.org/10.1016/j.energy.2023.129547>.
- [26] G. Chai, Y. Wang, G. Zhu, Z. Wu, F. Markert, Experimental study on the effect of dry-water materials on the fire extinguishing efficiency and suppression mechanism of wood crib fire, *Fire and Materials*. 2024 Jun;48(4):469-82. <https://doi.org/10.1002/fam.3196>.
- [27] Z. Tianwei, Z. Shishun, L. Hao, X. Dengyou, G. Zidong, Z. Cunwei, Experimental research on combustible gas/air explosion inhibition by dry-water, *International Journal of Hydrogen Energy*. 2023 Dec 1;48(93):36605-20. <https://doi.org/10.1016/j.ijhydene.2023.06.053>.
- [28] C. Xue, H. Jiang, C. Zhu, W. Gao, A novel dry-water with perfluorohexanone for explosion suppression of AlH₃, *Chemical Engineering Science*. 2023 May 5;271:118575. <https://doi.org/10.1016/j.ces.2023.118575>.
- [29] C. Cai, Y. Su, Y. Wang, W. Ji, Suppressive effects of potassium salt modified dry-water material on hydrogen/methane mixture explosion, *International Journal of Hydrogen Energy*. 2024 Aug 19;79:537-50. <https://doi.org/10.1016/j.ijhydene.2024.07.018>.
- [30] G. Dou, C. Wang, C. Yan, L. Zhang, L. Gao, G. Liu, T. Zhang, J. Wang, J. Wang, Lignin-Based Hydrogel Reinforced Dry-water as Inhibitor for Coal Spontaneous Combustion, *Combustion Science and Technology*. 2023 May 17:1-9. <https://doi.org/10.1080/00102202.2023.2214691>.
- [31] X. Zheng, Z. Kou, S. Liu, G. Cai, P. Wu, Y. Huang, Z. Yang, Preparation and properties of a new core-shell-modified gel dry-water powder. *Powder Technology*. 2023 May 15;422:118493. <https://doi.org/10.1016/j.powtec.2023.118493>.
- [32] Y.Y. Wang, F.H. Zhu, H.L. Zhou, S.L. Chu, J.C. Jiang, A.C. Huang, Investigation in the fire suppression properties of KHCO₃ and K₂C₂O₄ dry-water incorporates core-shell structures, *Journal of Loss Prevention in the Process Industries*. 2024 Feb 1;87:105205. <https://doi.org/10.1016/j.jlp.2023.105205>.
- [33] Z. Han, Y. Zhang, Z. Du, F. Xu, S. Li, J. Zhang, New-type gel dry-water extinguishants and its effectiveness, *Journal of Cleaner Production*. 2017 Nov 10;166:590-600. <https://doi.org/10.1016/j.jclepro.2017.08.005>.
- [34] Y. Liu, R. Chen, S. Guo, Z. Wang, R. Pan, Modification and Application Performance Study of Ultra-Fine Dry Powder Extinguishing Agent, *Molecules*. 2024 Aug 12;29(16):3830. <https://doi.org/10.3390/molecules29163830>.
- [35] E. Lee, H. Son, Y. Choi, Elucidating the effects of particle sizes on the fire extinguishing performance of
-

-
- core-shell dry-water, Korean Journal of Chemical Engineering. 2020 Oct;37:1642-8.
<https://doi.org/10.1007/s11814-020-0632-0>.
- [36] W. Zhang, J. Jia, J. Zhang, Y. Ding, J. Zhang, K. Lu, S. Mao, Pyrolysis and combustion characteristics of typical waste thermal insulation materials, Science of The Total Environment. 2022 Aug 15;834:155484.
<https://doi.org/10.1016/j.scitotenv.2022.155484>.
- [37] D. Kumar, M. Alam, P.X. Zou, J.G. Sanjayan, R.A. Memon, Comparative analysis of building insulation material properties and performance, Renewable and Sustainable Energy Reviews. 2020 Oct 1;131:110038.
<https://doi.org/10.1016/j.rser.2020.110038>.
- [38] H.H. Liang, M.C. Ho, Toxicity characteristics of commercially manufactured insulation materials for building applications in Taiwan, Construction and Building Materials. 2007 Jun 1;21(6):1254-61.
<https://doi.org/10.1016/j.conbuildmat.2006.05.051>.